Research Article

Corrosion Behavior of AA70 Reinforced *Zea mays* Husk Particle in $NaCl/H_2SO_4$ Concentrations

Oluwasegun Falodun*
Department of Mechanical Engineering, Covenant University, Ota, Nigeria
School of Chemical and Metallurgical Engineering, University of the Witwatersrand, Johannesburg, South Africa

Roland Loto
Department of Mechanical Engineering, Covenant University, Ota, Nigeria

* Corresponding author. E-mail: oefalodun@gmail.com DOI: 10.14416/j.asep.2023.08.001
Received: 23 March 2023; Revised: 20 April 2023; Accepted: 1 June 2023; Published online: 8 August 2023

Abstract
The effects of *Zea mays* husk particle and heat treatment on the corrosion behavior of AA70 matrix composite in 1.5 wt.% NaCl/0.0125 M H_2SO_4 concentrations were studied using an electrochemical technique and optical microscopy. Results showed that the samples had similar anodic-cathodic polarization behavior after heat treatment, with no passivation. However, the heat-treated AA70 matrix composites were more corrosion-resistant than the untreated AA70 matrix composite material in 1.5 wt.% NaCl/0.0125 M H_2SO_4 concentrations. The composite with 15 wt.% *Zea mays* husk and a particle size of 300 µm reinforced AA70 matrix revealed the least corrosive tendency and is the most thermodynamically stable in chloride and sulphate ions conditions. Therefore, the corrosion behavior of heat-treated AA70 matrix composites was better compared to that of AA70 material in 1.5 wt.% NaCl/0.0125 M H_2SO_4 solution. Furthermore, the presence of a high concentration of aggressive chloride ions increases the corrosion susceptibility, and the *Zea mays* husk particle breaks down the stable oxide film, resulting in increased chloride ion adsorption. The optical microscopy examination suggested the presence of localized corrosion on the material surface.

Keywords: AA70 matrix composite, Corrosion, Heat treatment, Sodium chloride, Sulphuric acid, *Zea mays* husk particle

1 Introduction

Aluminium matrix composites have become increasingly prevalent and attractive for numerous applications due to their superior mechanical properties over primary aluminium alloys, such as low density, high strength, stiffness, wear resistance improvement, low thermal expansion coefficient, and other exceptional properties, particularly in automotive, aerospace, vessels, and defense applications [1]–[3]. For many reasons, ceramic particles such as Al_2O_3, SiC, TiC, TiN, and B_4C are often utilized in reinforcing aluminium matrices because of their exceptional qualities, minimal rates of purpose, and availability [4]–[8]. Integrating these various ceramic materials may improve mechanical properties significantly. Nevertheless, the primary application of the composite dictates the choice of aluminium reinforcement [9].

The arrangement of the dispersed particles within the primary material greatly influenced the composite mechanical and physical properties. The purpose of the reinforcement is to increase the matrix material resistance to impact load. As a result, it will aid the main matrix in integrating the reinforcement and distributing external loads. Consequently, the ability of the second phase to directly interact with the main matrix of the composite material is critical in developing a suitable system that will allow optimal

load distribution from the matrix to the reinforcements [10]. However, the shape, dispersion, and size distribution of the reinforcement phase are the factors that influence the desirable properties of composite materials [11]. The ceramic material phases are difficult to disperse because they are not readily soluble in the matrix, which results in poor interaction bond formation when used as the strengthening phase [12]. Furthermore, the presence of these precipitated particles may promote the formation of pitting corrosion. It has been reported that intergranular attack and stress corrosion can occur if the precipitate particles are located on or near the grain boundaries [13], [14].

Heat treatment is proven to change microstructures by dissolving and homogenizing soluble phases, thereby strengthening and preventing a systemic collapse of composites. Heat treatment is necessary to improve the strengthening mechanism in aluminium matrix composites, which results in formability and corrosion resistance [15].

According to the findings, the microstructural characteristics of aluminium matrix composite usually influence corrosion resistance. The metal attraction to improve the corrosion resistance is primarily determined by the cooling solidification rate, which affects solid particle redistribution, particle dendrite shape, and electrochemical behavior [1]. Sravanthi and Manjunatha studied the electrochemical behaviour of heat-treated Al7075 combined with silicon carbide (SiC) and graphite in acid chloride, sulphate, and nitrate solutions. They discovered that the corrosion rate in aluminium matrix composites is relatively lower in heat-treated samples than in as-cast samples in all solution concentrations [16]. Loto investigated the effect of silicon carbide content in Al 1070 in a chloride solution. The results showed that the aluminium composite reinforced with 10 wt.% silicon carbide has the least corrosion rate. Further research into the effect of silicon carbide particle sizes (3, 9, 29, 45 microns) on electrochemical behavior revealed that the aluminium matrix composite with a 3 μm had the least corrosion rate, despite the fact that all samples examined formed a protective layer. Meanwhile, the potential corrosion shifted as the particle size of silicon carbide increased due to the dominant reduction of redox processes associated with localized corrosion and the diminishing protective film layer [17]. Rao and Ramanaiah investigated the corrosion and mechanical characteristics of a heat-treated AA6061/MoS_2 matrix composite. The material strength and localized protection against corrosion continued with further improvement as the dispersed phase rose to around 4 wt.% MoS_2; however, adding more than 4 wt.% MoS_2 caused a decrease [18]. Alaneme and Bodunrin [19] investigated the influence of heat treatment on aluminium alloys strengthened with varying proportions of aluminium oxide, as well as electrochemical tests on AA6063 matrix composites. They reported that AA6063 strengthened with aluminium oxide had better corrosion resistance in sodium chloride (NaCl) than in sodium hydroxide or sulphuric acid (NaOH/H_2SO_4). However, the electrochemical behaviour of the AA6063 material was superior to that of the AA6063 matrix composite in sodium chloride and hydroxide concentrations. In contrast, the AA6063 matrix composite proved more resistant to corrosion in a sulphuric acid environment. Akinwamide *et al.* investigated the effect of ferrotitanium and silicon carbide on the corrosion behavior of stir-cast aluminium matrix composites and discovered that specimens reinforced with particles of 5% SiC +2% TiFe and 5% SiC had the best corrosion resistance from potentiodynamic polarization. Furthermore, the aggressive effect of the chloride ions present in the test electrolyte was attributed to the formation of a filiform structure on the surface of the unreinforced aluminium alloy and several pits on the surface of the composites [20]. Srinath *et al.* synthesized Al-6082/15% nano-SiC composite and studied the effects of heat treatments on corrosion behaviour. They discovered that the corrosion rate decreased as the NaCl concentration increased. Meanwhile, the corrosion initiations and rates were found to be minimal in samples heated to 500 °C [21].

Nowadays, the most commonly used agricultural residues for reinforcing materials are residues from combustion and refinement processes, such as rice husks, nut shells, coconut shells, and wood [22]. These agricultural wastes contain a high concentration of silica and other refractory oxides. Additionally, the density of these agricultural wastes is lower than that of chemically synthesized reinforcements like silicon carbide and alumina [23]. Hence, incorporating agricultural wastes into aluminium alloys is expected to promote the use of low-cost waste byproducts and make aluminium products more affordable. According

to research findings, agro waste derivatives products serves as a potential material for the economical manufacturing of aluminium matrix composites [24]. Aluminium matrix composites were produced using the stir casting technique, which was then heat treated for corrosion studies. The electrochemical behavior of a heat-treated aluminium matrix composite with different particle sizes of *Zea mays* was investigated in this study.

2 Experimental Setup

2.1 *Materials and heat treatment process*

The *Zea mays* husk was acquired from a public market within Lagos state, Nigeria, in a dry form and after fourteen (14) days of storage was treated. The *Zea mays* husk was dried in an oven at 100 °C, then milled and sieved to remove uneven granules and retain particles with similar size distributions of 150 and 300 microns. The aluminium matrix composite was produced in the foundry section of Covenant University, Mechanical Engineering Department in Ota, Nigeria. The stir casting technique is utilized in this study to develop the aluminium matrix composite. A melting furnace with a graphite chamber of 20 kg capacity was used to melt AA70 for one (1) hour at 680 °C with additions of 5–15 wt.%. *Zea mays* husk particle sizes of 150 and 300 µm were added to molten AA70 matrix composite at a vortex of 500 rpm (mechanically stirred) before being cast into an already prepared mould cavity and allowed to cool for an entire day. The result revealed that the AA70 composite reinforced with *Zea mays* husk particles had a cylindrical structure, with a surface area of 1 cm^2 and a height of 3 mm. The molten aluminium temperature was measured using the temperature sensor (K-type). Table 1 shows the composition mixture of different *Zea mays* husk particle sizes into aluminium AA70 alloys.

Table 1: The description of AA70 reinforced with *Zea mays* (wt.% content)

Samples	Description	Zea Mays sizes
A	AA70	-
B	5 wt.%	150 µm
C	5 wt.%	300 µm
D	15 wt.%	150 µm
E	15 wt.%	300 µm

The aluminium matrix composites were precisely cut into length (1 cm), breadth (1 cm), and thickness (1 cm) dimensions for each sample using a cutting machine. Five (5) as-cast composites were not heat heated, whereas the remaining composite was heat-treated in a muffle furnace using an annealing and quenching media heat treatment process. The aluminium composite was heated to 350 °C and held at that temperature for 30 min before being quenched with distilled water. The muffle furnace temperature was measured with a thermocouple and maintained with a control dial with a ±10 °C accuracy.

2.2 *Preparation of aluminium-matrix composite samples*

The aluminium matrix composite surfaces were prepared using the metallography technique and abrasive grinding papers of various grit (80–2,000 SiC) sizes to achieve smooth surfaces. The samples were then polished with diamond suspensions (up to 1 µm), and the surfaces were thoroughly washed with deionized water and dried using dimethyl ketone before conducting the weight loss analysis and electrochemical test following ASTM G1-03(2011).

2.3 *Corrosion behavior evaluation*

Potentiodynamic polarization experiments were carried out using a Digi-Ivy 2311 terminal connected to a desktop device. The experimental setup includes a three-electrode electrochemical cell with 250 mL of electrolyte solution, a reference electrode (Ag/AgCl), a counter electrode made of a platinum rod, and the heat-treated AA70 matrix composite as a working electrode (surface area of 1 cm^2). The AA70 matrix composites were exposed to electrolyte solutions (NaCl and H_2SO_4) at ambient temperature.

Titan Biotech Ltd in India supplied recrystallized NaCl at 1.5 wt.% in 0.0125 M H_2SO_4. The corrosion potential was measured for 1700 seconds at 0.05 V/s potential difference to investigate the alloy's thermodynamic stability at rest potentials. The polarization curves were done using an initial potential of –1.4 and a final potential of +0.75 V at a scan rate of 0.0015 V/s. The potentiodynamic curve technique was applied to determine the current density i_{corr} (C_d) and potential E_{corr} (C_P). However, the rate of corrosion

(C_R) was evaluated using the mathematical relationship approach from Equation (1);

$$C_R = \frac{0.003272 \times Cd \times Eqv}{D} \quad (1)$$

Where, D is the density of the material (g/cm^3); Eqv is the material equivalent weight in grams; The constant value for the corrosion rate is 0.003272.

2.4 *Surface characterization of corroded AA70 matrix composite*

The corroded surface morphology of the AA70/*Zea mays* husk samples after the electrochemical test was examined using an Omax trinocular microscope connected to a ToupCam analyzer package.

3 Results and Discussion

3.1 *Potentiodynamic corrosion test*

The typical potentiodynamic polarization curves of the AA70 reinforced with *Zea mays* husk particle composites in 1.5 wt.% NaCl/0.0125 M H_2SO_4 solution is shown in Figure 1. The aluminium matrix composite reinforced with *Zea mays* husk exhibited an active behavior of the anodic-cathodic polarization curves due to the sudden breakdown of the protective oxide film; thus, no passivation occurred in the entire material, as shown in Figure 1. The results show that as the proportion of *Zea mays* husk particles increased, the surface oxide layer deteriorated. The combined effect of Cl and SO_4^{2-} ions in 1.5 wt.% NaCl/0.0125 M H_2SO_4 solution had the most detrimental impact on AA70 alloy and AA70/*Zea mays* husk aluminium composites, it is due to the synergetic effect during the oxidation and reduction reactions at the interface region of the metallic and composite materials. The AA70 alloy (sample A) had the least corrosion rate in the solution, indicating that it has the lowest relatively uniform surface characteristics to corrode in 1.5 wt.% NaCl/0.0125 M H_2SO_4 solution. According to Table 2, sample B had the highest corrosion rate, indicating that *Zea mays* particles interact with the formation or repassivation of the passive film layer, resulting in a significant deterioration of the surface properties for the AA70 matrix composite.

The AA70 reinforced with *Zea mays* husk particle composites potentiodynamic polarization curves of heat-treated in 1.5 wt.% NaCl/0.0125 M H_2SO_4 solution are presented in Figure 2. It is seen that they exhibit similar behavior of anodic-cathodic polarization without no passivation occurrence after the heat treatment process as shown in Table 3, the corrosion rate was decreased for samples C, D and E. The corrosion behavior of heat-treated AA70 matrix composites was better compared to that of AA70 material in 1.5 wt.% NaCl/0.0125 M H_2SO_4 solution. This indicates that the particles in the matrix would have been distributed evenly after heat treatment [25].

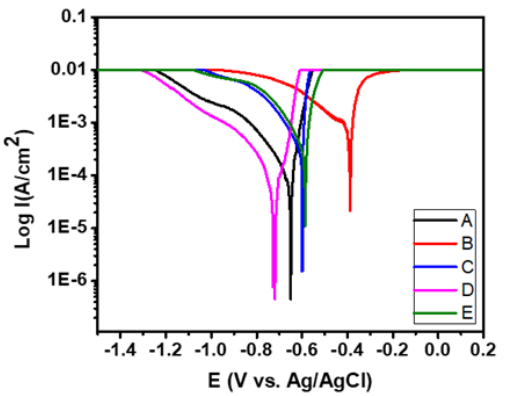

Figure 1: Potentiodynamic Polarization plots of as-cast AA70 with *Zea mays* husk particles.

It was also observed that the Icorr value for the aluminium matrix composites subjected to heat treatment was less than the untreated composites. This indicates that the heat treatment process improves the corrosion resistance of the composite. In addition, the formation of the Al_2O_3 layer phase and another intermetallic (Al_4C_3) on the uppermost part must have hindered chloride and molecules from entering the interstitial sites of the AA70 matrix composite, thus preventing corrosion [26]. However, as reinforcement increases, the corrosion rate decreases. The localized corrosion of the AA70 matrix composite shifts to the negative region. The observed pitting corrosion suggested that pitting begins at random sites of distortions on the matrix alloy protective oxide film, whereas pits around the reinforcement particles interact to form cracks/void space in composite materials. Because the crevices are active, they will cathodically protect the matrix and reduce pit formation and propagation.

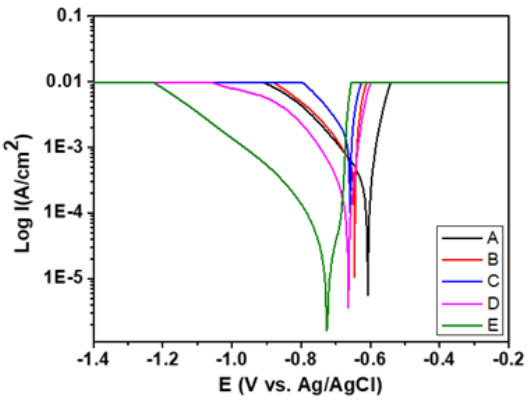

Figure 2: Potentiodynamic polarization plots of heat-treated AA70 with *Zea mays* husk particles.

The results show that higher concentrations of chloride ions lead to higher cathodic open circuit potential values, indicating accelerated chloride anions absorption through the pores in both the matrix and reinforcement phases, allowing the surface protective film layers to break down [27]. This supports previous research findings that chloride ions have a greater ability to penetrate aluminium's passive hydrated oxides and reduce the kinetics of oxide film restoration [28]. The corrosion current density (icorr) and the corrosion rate decrease as the *Zea mays* husk particle content increases. The formation of solid adhesive bonding between *Zea mays* and aluminium alloy could explain the improved corrosion resistance of sample E over aluminium alloy. Tables 2 and 3 display the electrochemical behaviour results of AA70 alloy and aluminium matrix composite samples.

3.2 *Open circuit potential against time*

Figure 3 depicts the potential of the AA70 matrix composite as a function of time after exposure to a solution containing 1.5 wt.% NaCl and 0.0125 M H_2SO_4. The corrosion potential of all samples varies constantly throughout. As a result, the sample fluctuation behavior is subjected to repeated protective passive occurrence and breakup due to corrosive interaction [29]. However, sample E has the highest open circuit potential compared to samples A and B. This demonstrates that sample E has the least corrosive tendency and is the most thermodynamically stable. In contrast, this shows that sample E is more highly resistant to corrosion in the predominance of chloride and sulfuric acid anions [30]. With increasing volume content and particle size, the potential rate gradually increases and exhibits significant interference, indicating pitting occurrence.

Figure 4 depicts the open circuit potential of the heat-treated AA70 matrix composite in 1.5 wt.% NaCl/0.0125 M H_2SO_4 concentrations. Sample E has the highest open circuit potential and the most stable behavior. This means that sample E has the lowest thermodynamic corrosive tendency. Potential transients dominate the open circuit potential behavior for sample B due to the combined debilitating action of

Table 2: Polarization curve parameters of as-cast AA70 with *Zea mays* husk particles

MH Content	Corrosion Rate (mm/y)	Corrosion Current (A)	Corrosion Current Density (A/cm^2)	Corrosion Potential (V)	Polarization Resistance, R_p (Ω)	Cathodic Tafel Region, B_c (V/dec)	Anodic Tafel Region, B_a (V/dec)
A	2.106	1.94E-04	1.94E-04	–0.650	132.30	–6.217	19.060
B	10.656	9.82E-04	9.82E-04	–0.392	14.09	–2.749	2.743
C	9.776	9.01E-04	9.01E-04	–0.662	25.52	–7.314	0.368
D	7.808	7.20E-04	7.20E-04	–0.719	37.00	–7.110	31.350
E	6.573	6.06E-04	6.06E-04	–0.590	58.36	–7.226	5.107

Table 3: Polarization curve parameters of heat-treated AA70 with *Zea mays* husk particles

MH Content	Corrosion Rate (mm/y)	Corrosion Current (A)	Corrosion Current Density (A/cm^2)	Corrosion Potential (V)	Polarization Resistance, R_p (Ω)	Cathodic Tafel Region, B_c (V/dec)	Anodic Tafel Region, B_a (V/dec)
A	6.322	5.83E-04	5.83E-04	–0.607	44.09	–6.592	1.383
B	6.692	6.17E-04	6.17E-04	–0.631	41.65	–7.548	10.680
C	0.613	5.65E-05	5.65E-05	–0.759	454.80	–6.337	13.300
D	0.487	4.49E-05	4.49E-05	–0.604	573.66	–8.437	0.956
E	0.383	3.53E-05	3.53E-05	–0.725	727.80	–7.972	7.766

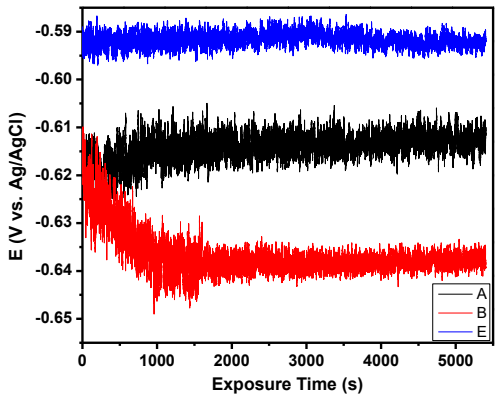

Figure 3: OCP with time for the as-cast AA70 matrix composites.

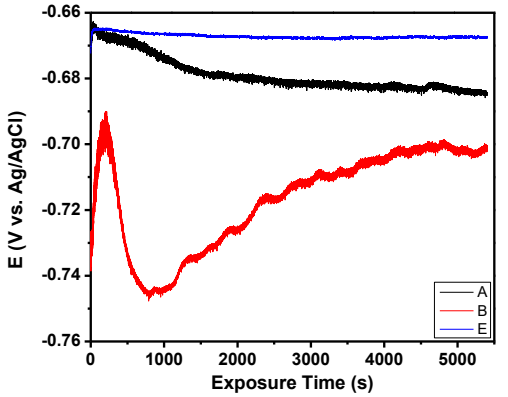

Figure 4: OCP with time for the heat-treated AA70 matrix composites.

chloride/sulphate anions which significantly makes them thermodynamically unstable [30]. The increased corrosion susceptibility is caused by the breakdown of a stable oxide film on the AA70 matrix composite due to increased chloride ion adsorption, which results in higher cathodic open potential values. There is a significant level of chloride ion absorption into the passive hydrated oxides of the interstitial spaces of aluminium matrix composite, as well as a decrease in the kinetics of oxide film recovery [28].

3.3 *Microstructural analysis of corroded surfaces*

The optical micrographs of AA70/*Zea mays* husk particles for untreated and heat-treated composite in electrochemical behavior are shown in Figures 5 and 6. The combined effect of chloride and sulphate ions resulted in a significant breakdown, as shown in Figure 6(b). The surface morphology of heat-treated AA70/*Zea mays* husk particles prior to the test is shown in Figure 7. The degree of surface morphology damage after heat treatment was relatively insignificant in Figure 8. As a result, hard particles can act as corrosion insulators on the

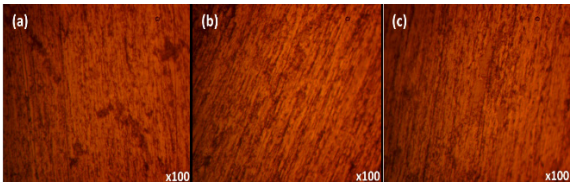

Figure 5: Corrosion morphology of as-cast AA70/*Zea mays* husk particle before corrosion test; (a) AA70 alloy, (b) 5% and (c) 15%.

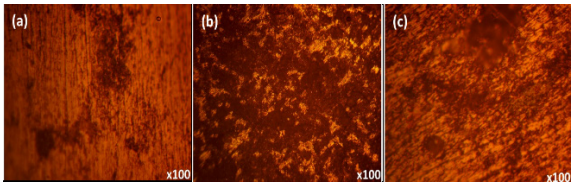

Figure 6: Corrosion morphology of as-cast AA70/*Zea mays* husk particle after corrosion test; (a) AA70 alloy, (b) 5% and (c) 15%.

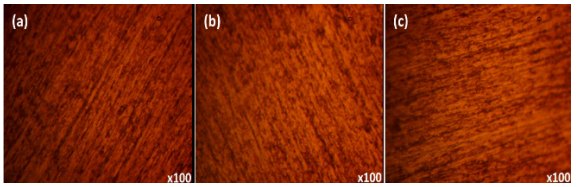

Figure 7: Corrosion morphology of heat-treated AA70/*Zea mays* husk particle before corrosion test; (a) AA70 alloy, (b) 5% and (c) 15%.

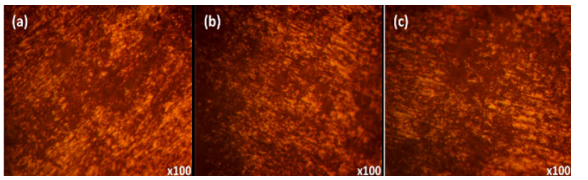

Figure 8: Corrosion morphology of heat-treated AA70/*Zea mays* husk particle after corrosion test; (a) AA70 alloy, (b) 5% and (c) 15%.

AA70 matrix material [31]. However, corrosion pits are common on metal surfaces due to localized corrosion reactions of Cl- ions, particularly, where there are imperfections, internal defects, and instabilities in the protective film layer. Pitting has been suggested to form due to Cl- anion deposition and chemical transformation at surface oxide film imperfections [32]. The heat-treated samples exhibited a slight film layer breakdown and pitting corrosion, particularly in AA70/5 wt.% *Zea mays* husk particles. This behavior is caused by the high corrosion rate and slow cooling of the samples during heat treatment, which causes contamination and elements meant to improve its properties then precipitate and dispersed from the solid solution to the intergranular zone, tiny porosity and insoluble particles, dislocations, and other internal defects in the aluminium structure [33]. The intensity of the attack confirmed the corrosive medium aggressive nature.

4 Conclusions

The effect of heat treatment on the corrosion behavior of an aluminium matrix composite with *Zea mays* husk particles produced using the stir casting technique was studied in chloride and sulphuric concentrations. The polarization curves for the aluminium matrix composite reinforced with *Zea mays* husk demonstrated active behavior due to the sudden breakdown of the protective oxide film, and no passivation took place throughout the material. The combination of chloride and sulphate anions solution had the most detrimental effect on the entire composites. However, heat-treated composites had better corrosion resistance than untreated composites. Regardless of the presence of Cl- and SO_4^{2-} ion concentrations in the aluminium matrix composite, Sample E exhibited the least corrosive tendency due to the lowest energy state (thermodynamically stable). The increased corrosion susceptibility of the aluminium matrix and *Zea mays* husk particle in the presence of a significant level of intense chloride ion is most likely due to the disintegration of the stable oxide film, resulting in increased chloride ion adsorption. However, the micrographs revealed evidence of localized corrosion.

Acknowledgements

The authors would like to thank Covenant University, Ota, Nigeria for their financial assistance and research facilities. Also, the School of Chemical and Metallurgical Engineering, University of the Witwatersrand, Johannesburg, South Africa for their support.

Author Contributions

O.F.: conceptualization, investigation, writing an original draft, reviewing and editing; R.L.: investigation, methodology, data curation, writing—reviewing and editing. All authors have read and agreed to the published version of the manuscript.

Conflicts of Interest

The authors declare no conflict of interest.

References

[1] R. R. Veeravalli, R. Nallu, and S. M. M. Mohiuddin, "Mechanical and tribological properties of AA7075–TiC metal matrix composites under heat treated (T6) and cast conditions," *Journal of Materials research and Technology*, vol. 5, pp. 377–383, 2016.

[2] V. Umasankar, M. A. Xavior, and S. Karthikeyan, "Experimental evaluation of the influence of processing parameters on the mechanical properties of SiC particle reinforced AA6061 aluminium alloy matrix composite by powder processing," *Journal of Alloys and Compounds*, vol. 582, pp. 380–386, 2014.

[3] J. P. Davim, *Metal Matrix Composites: Materials, Manufacturing and Engineering*. Berlin, Germany: De Gruyter, 2014.

[4] O.E. Falodun, S.R. Oke, F.V. Adams, S.O. Akinwamide, O. O. Ige, T. Tshephe, and P. A. Olubambi, "Fabrication and microstructural characterization of nanoparticle tin reinforced al-mg-si matrix composite," *Materials Today: Proceedings*, vol. 18, pp. 3209–3217, 2019, doi: 10.1016/j.matpr.2019.07.197.

[5] S. O. Akinwamide, S. M. Lemika, B. A. Obadele, O. J. Akinribide, O. E. Falodun, P. A. Olubambi,

and B. T. Abe, "A nanoindentation study on Al (TiFe-Mg-SiC) composites fabricated via stir casting," *Key Engineering Materials*, vol. 821, pp. 81–88, 2019.

[6] A. Hamdollahzadeh, M. Bahrami, M. F. Nikoo, A. Yusefi, M. K. B. Givi, and N. Parvin, "Microstructure evolutions and mechanical properties of nano-SiC-fortified AA7075 friction stir weldment: The role of second pass processing," *Journal of Manufacturing Processes*, vol. 20, pp. 367–373, 2015.

[7] A. Thangarasu, N. Murugan, and I. Dinaharan, "Production and wear characterization of AA6082-TiC surface composites by friction stir processing," *Procedia Engineering*, vol. 97, pp. 590–597, 2014.

[8] N. Yuvaraj and S. Aravindan, "Fabrication of Al5083/B_4C surface composite by friction stir processing and its tribological characterization," *Journal of Materials Research and Technology*, vol. 4, pp. 398–410, 2015.

[9] V. Chak, H. Chattopadhyay, and T. L. Dora, "A review on fabrication methods, reinforcements and mechanical properties of aluminum matrix composites," *Journal of Manufacturing Processes*, vol. 56, pp. 1059–1074, 2020.

[10] J. Hashim, L. Looney, and M. S. J. Hashmi, "The enhancement of wettability of SiC particles in cast aluminium matrix composites," *Journal of Materials Processing Technology*, vol. 119, pp. 329–335, 2001.

[11] M. R. Ghomashchi and A. Vikhrov, "Squeeze casting: An overview," *Journal of Materials Processing Technology*, vol. 101, pp. 1–9, 2000.

[12] Z. Yuan, W. Tian, F. Li, Q. Fu, X. Wang, W. Qian, and W. An, "Effect of heat treatment on the interface of high-entropy alloy particles reinforced aluminum matrix composites," *Journal of Alloys and Compounds*, vol. 822, p. 153658, 2020.

[13] W. Zhang and G. S. Frankel, "Transitions between pitting and intergranular corrosion in AA2024," *Electrochimica Acta*, vol. 48, pp. 1193–1210, 2003.

[14] T.-S. Huang and G. S. Frankel, "Influence of grain structure on anisotropic localised corrosion kinetics of AA7xxx-T6 alloys," *Corrosion Engineering, Science and Technology*, vol. 41, pp. 192–199, 2006.

[15] D. K. Xu, N. Birbilis, D. Lashansky, P. A. Rometsch, and B. C. Muddle, "Effect of solution treatment on the corrosion behaviour of aluminium alloy AA7150: Optimisation for corrosion resistance," *Corrosion Science*, vol. 53, pp. 217–225, 2011.

[16] M. Sravanthi and K. G. Manjunatha, "Corrosion Studies of As Casted and Heat Treated Aluminium-7075 Composites," *Materials Today: Proceedings*, vol. 5, pp. 22581–22594, 2018.

[17] R. T. Loto, "Investigation of the influence of SiC content and particle size variation on the corrosion resistance of Al-SiC matrix composite in neutral chloride solution," *The International Journal of Advanced Manufacturing Technology*, vol. 101, pp. 2407–2413, 2019.

[18] E. S. Rao and N. Ramanaiah, "Influence of heat treatment on mechanical and corrosion properties of aluminium metal matrix composites (AA 6061 reinforced with MoS_2)," *Materials Today: Proceedings*, vol. 4, pp. 11270–11278, 2017.

[19] K. K. Alaneme and M. O. Bodunrin, "Corrosion behavior of alumina reinforced aluminium (6063) metal matrix composites," *Journal of Minerals and Materials Characterization and Engineering*, vol. 10, pp. 1153–1165, 2011.

[20] S. O. Akinwamide, O. J. Akinribide, and P. A. Olubambi, "Influence of ferrotitanium and silicon carbide addition on structural modification, nanohardness and corrosion behaviour of stir-cast aluminium matrix composites," *Silicon*, vol. 13, pp. 2221–2232, 2021.

[21] M. K. Srinath, J. Nagendra, K. D. Bopanna, S. S. Swamy, and M. Ravikumar, "Corrosion performance characteristics of heat treated Al-6082 with nano-SiC reinforcements," *Materials Letters*, vol. 322, p. 132512, 2022.

[22] L. Purushothaman and P. Balakrishnan, "Wear and corrosion behavior of coconut shell ash (CSA) reinforced Al6061 metal matrix composites," *Materials Testing*, vol. 62, pp. 77–84, 2020.

[23] B. Vinod, S. Ramanathan, V. Ananthi, and N. Selvakumar, "Fabrication and characterization of organic and in-organic reinforced A356 aluminium matrix hybrid composite by improved double-stir casting," *Silicon*, vol. 11, pp. 817–829, 2019.

[24] A. A. Adediran and M. Sriariyanun, "Applicability of Agro-Waste Materials in the Development of

Aluminium Matrix Composites for Transport Structures," *Applied Science and Engineering Progress*, vol. 16, p. 6634, 2023.

[25] S. Roseline and V. Paramasivam, "Corrosion behaviour of heat treated Aluminium Metal Matrix composites reinforced with Fused Zirconia Alumina 40," *Journal of Alloys and Compounds*, vol. 40, pp. 205–215, 2019.

[26] S. Kumar, A. Kumar, and C. Vanitha, "Corrosion behaviour of Al 7075/TiC composites processed through friction stir processing," *Materials Today: Proceedings*, vol. 15, pp. 21–29. 2019.

[27] M. Belkhaouda, L. Bazzi, R. Salghi, O. Jbara, A. Benlhachmi, B. Hammouti, and J. Douglad, "Effect of the heat treatment on the behaviour of the corrosion and passivation of 3003 aluminium alloy in synthetic solution," *Journal of Materials and Environmental Science*, vol. 1, pp. 25–33, 2010.

[28] H. C. A. Murthy, V. B. Raju, and C. Shivakumara, "Effect of TiN particulate reinforcement on corrosive behaviour of aluminium 6061 composites in chloride medium," *Bulletin of Materials Science*, vol. 36, pp. 1057–1066, 2013.

[29] K. K. Alaneme and P. A. Olubambi, "Corrosion and wear behaviour of rice husk ash—Alumina reinforced Al–Mg–Si alloy matrix hybrid composites," *Journal of Materials Research and Technology*, vol. 2, pp. 188–194, 2013.

[30] R. T. Loto and P. Babalola, "Effect of alumina nano-particle size and weight content on the corrosion resistance of AA1070 aluminum in chloride/sulphate solution," *Results in Physics*, vol. 10, pp. 731–737, 2018.

[31] S. Suresh, G. H. Gowd, and M. L. S. Devakumar, "Corrosion behaviour of Al 7075/Al_2O_3/SiC MMNCs by weight loss method," *Journal of Bio-and Tribo-Corrosion*, vol. 4, pp. 1–6, 2018.

[32] L. H. Hihara and R. M. Latanision, "Corrosion of metal matrix composites," *International Materials Reviews*, vol. 39, pp. 245–264, 2018.

[33] T. Croucher, "Quenching of aluminum alloys: what this key step accomplishes," *Heat Treating*, vol. 14, pp. 20–21, 1982.